Fused-ring and linking group effects of proton donors and acceptors on simple H-bonded liquid crystals

Hong-Cheu Lin[ab]; Ji-Mei Shiaw; Chin-Yi Wu; Chiitang Tsai

[a] National Chiao Tung University, [b] Chinese Culture University,

PLEASE SCROLL DOWN FOR ARTICLE

Fused-ring and linking group effects of proton donors and acceptors on simple H-bonded liquid crystals

HONG-CHEU LIN*†‡, JI-MEI SHIAW§, CHIN-YI WU§
and CHIITANG TSAI§

†Institute of Chemistry, Academia Sinica, Taipei, Taiwan, ROC
‡Department of Materials Science and Engineering,
National Chiao Tung University, Hsinchu, Taiwan, ROC
§Institute of Applied Chemistry, Chinese Culture University, Taipei, Taiwan, ROC

Two fused-ring structures, 6-decyloxy-2-naphthoic acid $C_{10}ONA$ (**3**) and 6-dodecyloxy-isoquinoline IS (**8**), were synthesized and utilized as proton donor and acceptor moieties to construct a series of simple mesogenic supramolecules. The other complementary hydrogen-bonded (H-bonded) moieties are benzoic acids, thiophenecarboxylic acid and pyridines containing different alkyl chain lengths connected by ether and ester linkages, i.e. 4-alkoxybenzoic acid C_nOBA (**1**), terephthalic acid monoalkyl ester C_nCOOBA (**2**), 2,5-thiophenedicarboxylic acid monodecyl ester $C_{10}COOTHA$ (**4**), 4-alkoxypyridine C_nOP (**6**) and isonicotinic acid alkyl ester C_nCOOP (**7**). Several series of simple mesogenic supramolecular dimers were constructed from 1:1 molar ratios of proton donors (C_nOBA, C_nCOOBA, $C_{10}ONA$ and $C_{10}COOTHA$) and proton acceptors (IS, C_nOP and C_nCOOP), though the proton acceptor C_nCOOP induced phase separation in all complexes. In order to investigate their fused-ring and linking group effects on the mesogenic properties of the H-bonded complexes, analogous simple supramolecular structures are compared. Supramolecular architecture and the distinct mesomorphism of these simple H-bonded liquid crystalline materials were confirmed by polarizing optical microscopy, DSC and powder X-ray diffraction experiments.

1. Introduction

The application of molecular recognition through hydrogen bonding has been widely explored in different areas, including the formation of new supramolecular liquid crystals [1–3]. Different molecular elements containing complementary fragments can be linked through non-covalent interactions, e.g. hydrogen bonding, to generate supramolecular liquid crystalline materials [4–9]. Supramolecular structures possessing different mesogenic properties from those of their original moieties can be obtained by complexation of proton donor and acceptor moieties. Many kinds of hydrogen bonds and building blocks have been developed in the hydrogen-bonded structures to produce liquid crystalline phases [5–10]. The self-assembly of carboxylic (or benzoic) acid and pyridyl fragments is most frequently used in the H-bonded structures. Kato *et al.* have demonstrated a series of short H-bonded mesogens containing only two single rings and one H-bond, which were built from 4-alkylpyridines and 4-alkoxybenzoic acids [11]. The purpose of their study was to obtain the simplest H-bonded complexes possessing mesogenic properties

near room temperature. However, only the nematic phase was seen in these H-bonded complexes, and very few simple H-bonded systems have so far been investigated. As we know, the simplest supramolecular liquid crystals are easier to study for the influence of their component segments, such as ring structures and linking groups, on their liquid crystalline properties. Thus, through this study of the simplest supramolecular liquid crystals, the effects of each component fragment on regular H-bonded liquid crystals may be developed.

In previous studies, we found that quinoline systems bearing fused-heterocyclic rings can be successfully applied to the mesogenic cores to improve the tilted SmC arrangement in their fully-covalent molecular structures [12, 13]. However, very few fused-heterocyclic systems have been used in supramolecular liquid crystals. Recently, we have developed a fused-heterocyclic ring containing sulphur hetero-atoms, viz. thienothiophene, as the proton donor in the H-bonded core [14]. Thus, fused-heterocyclic rings similar to the pyridyl unit containing a nitrogen hetero-atom with lone-pair electrons should be feasible proton acceptors. Just as the quinoline structure may be applied to the mesogenic core covalently, the isoquinoline structure is a useful H-bonded acceptor

*Author for correspondence; e-mail: HCL@chem.sinica.edu.tw

candidate for use in a H-bonded core. Recently we reported preliminary results regarding one class of novel isoquinoline-based supramolecular liquid crystals making use of the *N*-heterocyclic fused-ring structure as the H-bonded acceptor [15]. In order to understand the fused-ring (single or double) effects on the mesogenic properties of simple supramolecular liquid crystals, in this work we introduce fused-ring structures to the proton acceptor (isoquinoline) and/or to the proton donor (naphthoic acid). In addition, we present the linking group (e.g. ester and ether) effects of proton donors and acceptors on the simplest H-bonded liquid crystals.

At present, the most common rigid cores in supramolecular liquid crystals are linear structures with aromatic rings hydrogen-bonded through pyridyl and carboxylic acid moieties. We would now like to replace the pyridine group with the isoquinoline unit (*N*-heterocyclic fused-ring) to investigate the fused-heterocyclic effect on the formation of the H-bonded structures. Moreover, some supramolecular liquid crystals with non-linear structures are reported to reveal interesting mesomorphic properties; our previous work showed that angular supramolecules containing different bending sites provide the possibility of manipulating the mesomorphic properties of the complexes using angular H-bonded interactions [16, 17]. However, these H-bonded complexes contain only a single hydrogen bond in each system. Consequently, instead of adjusting the relative positions of the proton donor and acceptor moieties, the five-membered heterocyclic ring (e.g. thiophene) providing the kinked molecular structure is complexed into double H-bonded liquid crystals in our recent work [18]. We demonstrated the effect of the thiophene structure on the mesomorphism of double H-bonded supramolecules: the benefits of lowered melting temperatures and reduced packing efficiency resulting from the non-linear configuration and an extra dipole from the lone-pair electrons of the sulfur hetero-atom. H-bonded dimers containing thiophene heterocyclic rings are also now investigated. In order to conceive the mesogenic behaviour of the H-bonded fused-ring structures and to visualize the role of the heterocyclic moieties in these supramolecular dimers, a series of simple H-bonded complexes bearing benzene, naphthalene, thiophene, pyridine and isoquinoline units are compared.

2. Experimental
2.1. General methods

^{1}H and ^{13}C NMR spectra were recorded on a Bruker MSL 200 or 300 spectrometer (200 MHz or 300 MHz) from a CDCl$_3$ or DMSO-d$_6$ solution with TMS as the internal standard. Elemental analyses were carried out by Perkin Elmer 2400 CHN type instrument. Thermal transition temperatures and textures of all products were obtained from a Perkin-Elmer DSC-7 and Leitz Laborlux S polarizing optical microscope (POM) equipped with a THMS-600 heating stage. The heating and cooling rates were 10°C min^{-1} for all measurements unless mentioned. Powder X-ray diffraction (XRD) patterns were obtained from an X-ray diffractometer Siemens D-5000 (40 kV, 30 mA) fitted with a temperature controller TTK450. Nickel-filtered CuK$_\alpha$ radiation was used as an incident X-ray beam. H-bonded complexes were prepared by slow evaporation from THF solution of a mixture in 1:1 molar ratio of the H-bonded donor and acceptor moieties, followed by drying *in vacuo* at 60°C.

2.2. Synthesis

The chemical structures of donor and acceptor moieties and hydrogen-bonded complexes are shown in figures 1, 2 and 3. All samples were identified as the required materials and judged to be pure by ^{1}H and ^{13}C NMR spectroscopy and elementary analysis. The syntheses of proton donor 4-alkoxybenzoic acid C$_n$OBA (**1**) and proton acceptor 4-alkoxypyridine C$_n$OP (**6**) were described previously [16, 18]. The syntheses of other proton donors and acceptors are described below.
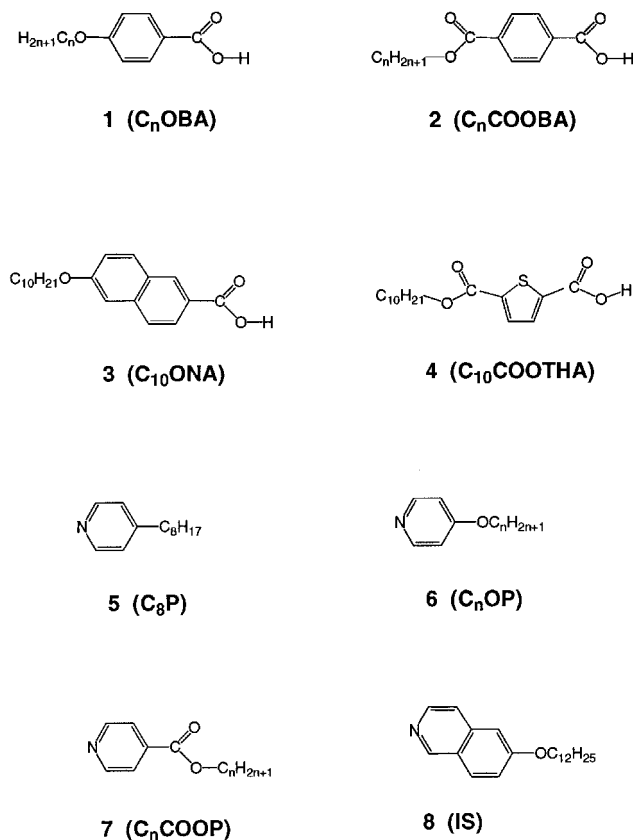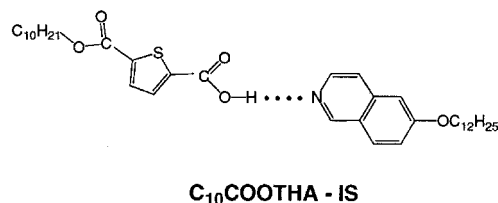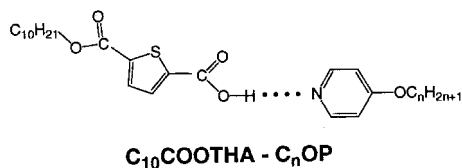
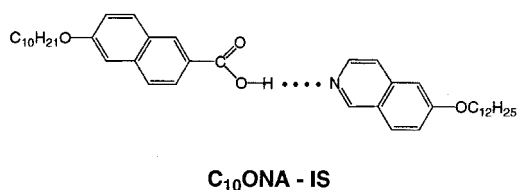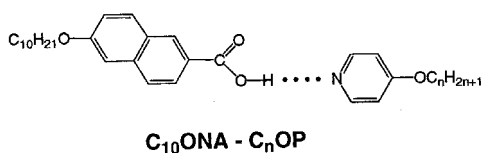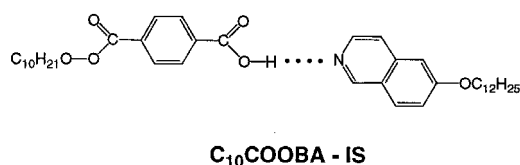

Figure 1. Donor (**1–4**) and acceptor (**5–8**) moieties.

Figure 2. Hydrogen-bonded complexes containing a single-ring (C_nOP) acceptor.
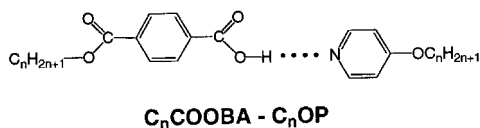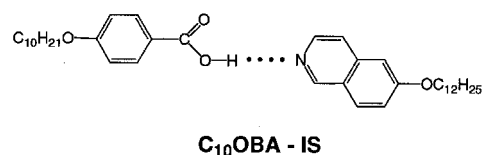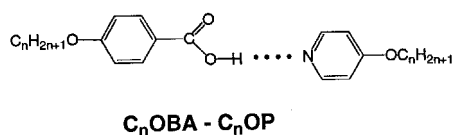

Figure 3. Hydrogen-bonded complexes containing a fused-ring (isoquinoline) acceptor.

2.2.1. *Terephthalic acid monoalkyl ester, $C_n COOBA$ (2)*

A solution of terephthalic acid (2.00 g, 12.0 mmol), 4-dimethylaminopyridine (0.15 g, 1.2 mmol), *N,N*-dicyclo-hexylcarbodiimide (2.48 g, 12.0 mmol), and octanol or decanol (12.0 mmol) in pyridine (100 ml) was stirred at room temperature for 24 h. The resulting solid was filtered off and washed with ethyl acetate; the combined solution was concentrated at reduced pressure. The crude products were purified by column chromatography on silica gel, using EtOAc/hexane (1/20) as eluent to give a white solid in 9–13% yield. The terephthalic acid monoalkyl esters C_nCOOBA (2) were identified as the required materials and judged to be pure by ^{1}H and ^{13}C NMR spectroscopy. The synthetic routes for terephthalic acid mono-octyl ester C_8COOBA and terephthalic acid monodecyl ester C_{10}COOBA have also been described in the literature [19, 20].

$C_8 COOBA$. ^{1}H NMR δ (CDCl$_3$): 0.88 (t, 3H, $J = 6.7$ Hz, CH$_3$), 1.25–1.45 (m, 10H, 5 × CH$_2$), 1.74–1.83 (m, 2H, CH$_2$), 4.35 (t, 2H, $J = 6.7$ Hz, OCH$_2$), 8.12–8.20 (m, 4H, Ar–H). ^{13}C NMR δ (CDCl$_3$): 14.0, 22.5, 26.0, 28.6, 29.1, 29.2, 31.7, 65.7, 129.5, 130.0, 133.0, 135.0, 165.7, 171.1. Elemental analysis for $C_{16}H_{22}O_4$: calcd C 69.04, H 7.97; found C 69.21, H 8.12%.

$C_{10} COOBA$. ^{1}H NMR δ (CDCl$_3$): 0.88 (t, 3H, $J = 6.6$ Hz, CH$_3$), 1.27–1.47 (m, 14H, 7 × CH$_2$), 1.74–1.84 (m, 2H, CH$_2$), 4.36 (t, 2H, $J = 6.6$ Hz, OCH$_2$), 8.12–8.20 (m, 4H, Ar–H). ^{13}C NMR δ (CDCl$_3$): 14.0, 22.6, 25.9, 28.6, 29.2, 29.5, 30.9, 31.8, 33.5, 65.7, 129.5, 130.0, 133.2, 134.8, 165.8, 170.5. Elemental analysis for $C_{18}H_{26}O_4$: calcd C 70.56, H 8.55; found C 70.46, H 8.72%.

2.2.2. *6-Decyloxy-2-naphthoic acid, $C_{10}ONA$ (3)*

6-Hydroxy-2-naphthoic acid (2.5 g, 13 mmol) and KOH (1.46 g, 26 mmol) were dissolved in ethanol/water (100 ml, 9/1) and the solution was stirred for 20 min; 1-bromodecane (7.17 g, 32.5 mmol) was then added and the mixture heated under reflux for 24 h. When the reaction was complete, KOH (0.73 g, 13 mmol) was

added and the mixture heated under reflux for a further 4 h. The ethanol was evaporated, and the mixture poured into water and acidified to approximately pH = 2 ∼ 3 with acetic acid. The precipitate was filtered and washed with water and ether, and then recrystallized from ethanol to give 71 ∼ 80% yield. The synthetic route for $C_{10}ONA$ has also been described in the literature [21].

^{1}H NMR δ (DMSO-d$_6$): 0.84 (t, 3H, J = 6.4 Hz, CH$_3$), 1.24–1.42 (m, 14H, CH$_2$), 1.73–1.80 (m, 2H, CH$_2$), 4.09 (t, 2H, J = 6.4 Hz, OCH$_2$), 7.08–7.24 (m, 1H, Ar−H), 7.38 (d, 1H, J = 3.38 Hz, Ar−H), 7.84 (d, 1H, J = 13.01 Hz, Ar−H), 7.88–7.94 (m, 1H, Ar−H), 7.99 (d, 1H, J = 13.58 Hz, Ar−H), 8.49 (s, 1H, Ar−H). ^{13}C NMR δ (CDCl$_3$): 14.16, 22.31, 25.73, 28.75, 28.90, 28.96, 29.16, 29.21, 31.49, 67.90, 106.72, 119.85, 125.77, 125.92, 127.12, 127.58, 130.56, 131.08, 136.96, 158.70, 167.83. Elemental analysis for $C_{21}H_{28}O_3$: calcd C 76.79, H 8.59; found C 76.76, H 8.47%.

2.2.3. *2,5-Thiophenedicarboxylic acid monodecyl ester,* $C_{10}COOTHA$ *(4)*

A solution of 2,5-thiophenedicarboxylic acid (1.5 g, 8.7 mmol), 4-dimethylaminopyridine (0.106 g, 0.87 mmol), *N*,*N*-dicyclohexylcarbodiimide (1.797 g, 8.7 mmol), and decanol (1.517 g, 9.58 mmol) in tetrahydrofuran (25 ml) was stirred at room temperature for 24 h. The resulting solid was filtered, washed with tetrahydrofuran, and the combined solutions concentrated at reduced pressure. The crude product was purified by column chromatography on silica gel, using hexane/EtOAc (1/1) as eluent to give a white solid in 16.5% yield.

^{1}H NMR δ (CDCl$_3$): 0.88 (t, 3H, J = 6.6 Hz, CH$_3$), 1.27–1.43 (m, 14H, 7 × CH$_2$), 1.71–1.80 (m, 2H, CH$_2$), 4.32 (t, 2H, J = 6.6 Hz, OCH$_2$), 7.76 (d, 1H, J = 3.93 Hz, thiophenyl−H), 7.82 (d, 1H, J = 4.12 Hz, thiophenyl−H). ^{13}C NMR δ (CDCl$_3$): 14.10, 22.67, 25.89, 28.55, 29.20, 29.28, 29.49, 31.87, 66.05, 133.01, 134.49, 137.67, 140.71, 161.52, 166.45. Elemental analysis for $C_{16}H_{24}O_4S$: calcd C 61.51, H 7.74; found C 61.43, H 7.71%.

2.2.4. *Isonicotinic acid alkyl ester, $C_n COOP$ (7)*

Isonicotinic acid (5 g, 40 mmol) and potassium carbonate (11.06 g, 80 mmol) were dissolved in acetone (150 ml) and *N*,*N*-dimethylformamide (20 ml). 1-Bromo-alkane (120 ml) was added to the mixture which was heated under reflux for 48 h, then cooled to room temperature. The solvent was removed under reduced pressure. The crude product was dissolved in dichloromethane and the solution washed with water and dried over anhydrous magnesium sulphate. The solvent was removed by evaporation and the residue was purified by column chromatography using silica gel with 35/1 hexane/EtOAc as eluent, giving ∼ 62% yields.

C_8COOP. ^{1}H NMR δ (CDCl$_3$): 0.85–0.92 (m, 3H, CH$_3$), 1.29–1.37 (m, 10H, 5 × CH$_2$), 1.70–1.81 (m, 2H, CH$_2$), 4.35 (t, 2H, J = 6.7 Hz, OCH$_2$), 7.83–7.86 (m, 2H, 2 × Pyridyl−H), 8.76–8.79 (m, 2H, 2 × Pyridyl−H). ^{13}C NMR δ (CDCl$_3$): 14.03, 22.59, 25.94, 28.57, 29.14, 29.17, 31.75, 65.95, 122.81, 137.67, 150.56. Elemental analysis for $C_{14}H_{21}NO_2$: calcd C 71.46, H 8.99, N 5.95; found C 71.32, H 9.32, N 5.67%.

$C_{12}COOP$. ^{1}H NMR δ (CDCl$_3$): 0.86 (t, 3H, J = 6.6 Hz, CH$_3$), 1.24–1.43 (m, 18H, 9 × CH$_2$), 1.71–1.80 (m, 2H, OCH$_2$*CH$_2$*), 4.33 (t, 2H, J = 6.7 Hz, OCH$_2$), 7.81–7.83 (m, 2H, 2 × Pyridyl−H), 8.75 (t, 2H, 2 × Pyridyl−H). ^{13}C NMR δ (CDCl$_3$): 14.05, 22.63, 25.90, 28.51, 29.17, 29.28, 29.45, 29.51, 29.57, 31.86, 65.92, 122.79, 137.62, 150.56, 165.12. Elemental analysis for $C_{18}H_{29}NO_2$: calcd C 74.18, H 10.03, N 4.81; found C 74.24, H 9.69, N 4.70%.

$C_{16}COOP$. ^{1}H NMR δ (CDCl$_3$): 0.88 (t, 3H, J = 6.6 Hz, CH$_3$), 1.26–1.44 (m, 26H, CH$_2$), 1.73–1.82 (m, 2H, CH$_2$), 4.35 (t, 2H, J = 6.7 Hz, OCH$_2$), 7.84–7.86 (m, 2H, 2 × Pyridyl−H), 8.78 (d, 2H, J = 5.42 Hz, 2 × Pyridyl−H). ^{13}C NMR δ (CDCl$_3$): 14.09, 22.66, 25.94, 28.55, 29.21, 29.33, 29.65, 31.90, 65.96, 122.82, 137.66, 150.54, 165.15. Elemental analysis for $C_{22}H_{37}NO_2$: calcd C 76.03, H 10.73, N 4.03; found C 76.0, H 10.86, N 4.02%.

2.2.5. *6-Dodecyloxyisoquinoline, IS (8)*

The synthetic route for 6-dodecyloxyisoquinoline IS (**8**) was followed as described in the literature [22]. A solution of 4-hydroxybenzaldehyde (6.1 g, 50 mmol), potassium hydroxide (7.0 g, 125 mmol), and 1-bromo-dodecane (32.2 g, 125 mmol) in 50 ml of EtOH/H$_2$O (9/1) was heated under reflux for 24 h. The precipitate was filtered and the solution concentrated at reduced pressure. The residue was added to water and the mixture extracted with CH$_2$Cl$_2$. The organic layer was dried with MgSO$_4$ and concentrated at reduced pressure. The crude product was purified by column chromatography on silica gel, using EtOAc/hexane (1/10) as eluent to give 4-dodecyloxybenzaldehyde as a pale yellow solid in 70% yield (10.2 g). A benzene (50 ml) solution of equimolar amounts of 4-dodecyloxybenzaldehyde (7.1 g, 37.5 mmol) and aminoacetaldehyde dimethyl acetal (3.9 g, 37.5 mmol) was heated under reflux overnight using a Dean–Stark trap. The solution was evaporated *in vacuo* and then twice more with added benzene; the viscous residue was dissolved in dry THF. This solution was cooled to − 10°C and 1 equiv of ethyl chloroformate (4.1 g, 37.5 mmol) was added with rapid stirring; the mixture was further stirred more than 5 min. The cooling bath was removed and 1.2 equiv of trimethyl phosphite (5.6 g, 45 mmol) was added with stirring. The mixture was stirred at room temperature for 15 h and then evaporated to an oily state. The oil was then evaporated

twice with added toluene to remove traces of trimethyl phosphite. The oily residue was dissolved in dry CH_2Cl_2, 6 equiv of titanium tetrachloride (24 ml, 225 mmol) was added, and the solution heated under reflux for 36 h under a drying tube. The cooled solution was shaken with 1 equiv of aqueous NaOH to neutrality, whereupon TiO_2 was precipitated as a white solid. The filtrate was extracted with 3N HCl, and this extract washed with CH_2Cl_2. It was made basic with aqueous alkali, and again extracted with CH_2Cl_2. This further treatment of the extract was followed by drying with $MgSO_4$ and evaporation of the organic phase. The crude product was purified by column chromatography on silica gel, using EtOAc/hexane (1/5) as eluent to give a yellow solid in 2.7% yield (0.32 g). 6-Dodecyloxyisoquinoline IS (**8**) was identified as the required product and judged to be pure by ^{1}H and ^{13}C NMR spectroscopy and elemental analysis.

^{1}H NMR δ (CDCl$_3$): 0.88 (t, 3H, $J = 6.8$ Hz, CH$_3$), 1.27–1.51 (m, 18H, 9 × CH$_2$), 1.81–1.90 (m, 2H, CH$_2$), 4.08 (t, 2H, $J = 6.4$ Hz, OCH$_2$), 7.03 (s, 1H, Ar–H), 7.22 (d, 1H, $J = 9.0$ Hz, Ar–H), 7.52 (d, 1H, $J = 5.6$ Hz, Ar–H), 7.84 (d, 1H, $J = 9.0$ Hz, Ar–H), 8.42 (d, 1H, $J = 5.6$ Hz, Ar–H), 9.09 (s, 1H, Ar–H). ^{13}C NMR δ (CDCl$_3$): 14.1, 22.7, 26.0, 29.0, 29.3, 29.5, 29.6, 31.9, 68.2, 104.5, 119.7, 120.6, 124.4, 129.2, 137.7, 143.4, 151.5, 160.4. Elemental analysis for $C_{21}H_{31}NO$: calcd C 80.46, H 9.97, N 4.47; found C 79.93, H 9.94, N 4.20%.

3. Results and discussion

All the proton donors (**1–4**) and acceptors (**5–8**) used in this work are shown in figure 1, and their thermal properties are given in table 1. The simple H-bonded dimer complexes were prepared from a mixture of these proton donors and acceptors in 1:1 molar ratio. The mesogenic properties of the complexes were characterized by polarizing optical microscopy (POM) and confirmed by X-ray diffraction (XRD). The orthogonal SmA phase was characterized by the focal-conic fan texture coexisting with the homeotropic alignment; the tilted SmC phase was characterized by the broken focal-conic fan texture coexisting with the schlieren texture; the nematic phase was characterized by the schlieren texture coexisting with the homeotropic alignment. The meso-morphism of the H-bonded dimer complex C$_8$OBA-C$_8$P (1:1 molar ratio) containing proton acceptor **5** (C$_8$P)

Table 1. Phase transition temperatures (°C)[a] and corresponding enthalpies (J g^{-1}), in parentheses, of constituents of hydrogen-bonded complexes, i.e. 4-octyloxybenzoic acid (C$_8$OBA), 4-decyloxybenzoic acid (C$_{10}$OBA), 4-octyloxycarbonylbenzoic acid (C$_8$COOBA), 4-decyloxycarbonylbenzoic acid (C$_{10}$COOBA), 6-decyloxy-2-naphthoic acid (C$_{10}$ONA), 5-decyloxycarbonyl-thiophene-2-carboxylic acid (C$_{10}$COOTHA), 4-hexadecyloxypyridine (C$_{16}$OP), 4-hexadecyloxycarbonylpyridine (C$_{16}$COOP) and 6-dodecyloxyisoquinoline (IS).

Compound	Cr		phase		phase		phase		I
C$_8$OBA	Cr	⇌ 73.8 (57.9) / 49.3 (54.3)	SmX	⇌ 101.7 (45.0) / 95.4 (44.1)	SmC	⇌ 108.2 (4.9) / 105.9 (4.9)	N	⇌ 148.1 (9.4) / 146.0 (9.5)	I
C$_{10}$OBA	Cr	⇌ 85.1 (58.9) / 69.4 (21.5)	SmX	⇌ 96.0 (30.3) / 90.2 (31.1)	SmC	⇌ 123.7 (4.5) / 120.5 (4.3)	N	⇌ 142.4 (7.7) / 139.6 (7.2)	I
C$_8$COOBA	Cr	⟶ 111.4 (89.4) / 99.6 (85.5)							I
C$_{10}$COOBA	Cr	⇌ 69.0 (31.7) / 41.3 (25.5)	SmX	⟵ 113.3 (97.0) / 104.7 (90.4)					I
C$_{10}$ONA	Cr	⇌ 104.8 (0.7) / 89.7 (1.7)	Cr′	⇌ 136.3 (39.4) / 120.3 (40.3)	SmC	⇌ 140.5 (2.9) / 138.4 (3.6)	N	⇌ 175.9 (7.7) / 173.3 (4.7)	I
C$_{10}$COOTHA	Cr	⟶ 104.8 (95.6) / 94.8 (97.7)							I
C$_{16}$OP[b]	Cr	⟶ 51.5 (166.1) / 30.8 (167.3)							I
C$_{16}$COOP[c]	Cr	⇌ 50.3 (168.2) / 32.6 (21.1)	Cr′	⟵ 50.3 (168.2) / 35.2 (135.2)					I
IS	Cr	⟶ 48.1 (124.2) / No crystallization to room temp.							I

[a] Abbreviations: Cr and Cr′ = crystalline phases, SmX = unidentified smectic phase, SmC = smectic C phase, N = nematic phase, I = isotropic liquid.
[b] C$_8$OP is liquid at room temperature; C$_{12}$OP: Cr 36.9°C (158.7 J g^{-1}) I (no crystallization upon cooling to room temp.).
[c] C$_8$COOP and C$_{12}$COOP are both liquid at room temperature.

was obtained from the literature [11] for comparison with analogous systems. Since phase separation occurred in all mixtures containing proton acceptor **7** (C_nCOOP), no H-bonded complexes formed and all results relating to C_nCOOP could not be compared.

The mesogenic properties of the analogous complexes C_8OBA-C_8P, C_8OBA-C_8OP and C_8COOBA-C_8OP are shown in table 2. Both C_8OBA-C_8P and C_8OBA-C_8OP show the nematic phase; however, C_8COOBA-C_8OP shows a monotropic SmA phase. Due to the lack of cooling data for C_8OBA-C_8P in the literature [11], we can only verify that C_8OBA-C_8OP shows a monotropic nematic phase. These results suggest that the insertion of the ether linkage of the pyridine (C_8OP) in C_8OBA-C_8OP has raised its clearing temperature compared with that in C_8OBA-C_8P. Regarding C_8OBA-C_8OP and C_8COOBA-C_8OP, the introduction of the ester linkage in the benzoic acid (C_8COOBA) has induced the SmA phase in C_8COOBA-C_8OP, instead of the nematic phase in C_8OBA-C_8OP. However, all these cases have narrow LC phase ranges ($4 \sim 6°C$).

The H-bonded dimer complexes bearing a single-ring (C_nOP) acceptor, i.e. C_{10}OBA-C_nOP, C_{10}COOBA-C_nOP, C_{10}ONA-C_nOP and C_{10}COOTHA-C_nOP (1:1 molar ratio, where $n = 8$, 12 and 16), are shown in figure 2. Their thermal and mesogenic properties are given in table 3. No complexes containing thiophene donors (i.e. C_{10}COOTHA-C_nOP) display any liquid crystalline phase; this is due to the short H-bonded angular structure. In contrast to the table 2 data, by increasing the flexible length of the acid (from $n = 8$ to $n = 10$) in complexes C_nOBA-C_8OP and C_nCOOBA-C_8OP, the mesomorphism shifts from the monotropic nematic phase in C_8OBA-C_8OP to the enantiotropic SmC phase in C_{10}OBA-C_8OP; whereas C_8COOBA-C_8OP has the same mesomorphism (i.e. the monotropic SmA phase) as C_{10}COOBA-C_8OP. Moreover, from the literature [11], both C_8OBA-C_8P and C_{10}OBA-C_8P show the same nematic phase. Consequently, the available data suggest that complexes C_nOBA-C_8OP ($n = 8$ and 10) containing double ether linkages favour both nematic

and SmC phases; complexes C_nCOOBA-C_8OP ($n = 8$ and 10) containing the ester linkage in the acid favour the SmA phase; and complexes C_nOBA-C_8P ($n = 8$ and 10) containing the ether linkage in the acid favour the nematic phase.

As we increase the flexible length of the single-ring (C_nOP) acceptor (from $n = 8$ to $n = 16$) in complexes C_{10}OBA-C_nOP, C_{10}COOBA-C_nOP and C_{10}ONA-C_nOP ($n = 8$, 12 and 16), the clearing temperatures and ranges of the mesophases are in the following order (table 3): C_{10}ONA-C_nOP > C_{10}OBA-C_nOP > C_{10}COOBA-C_nOP. Sequentially, complexes C_{10}ONA-C_nOP ($n = 8$, 12 and 16) containing the fused-ring acid have the highest clearing temperatures and widest ranges of mesophases, and complexes C_{10}COOBA-C_nOP ($n = 8$, 12 and 16) have the lowest clearing temperatures and the narrowest mesomorphism. For a shorter flexible length of the proton acceptor C_nOP ($n = 8$) in all systems of table 3, the SmA phase is favoured only in C_{10}COOBA-C_8OP, and the nematic phase only in C_{10}ONA-C_8OP containing the fused-ring donor (naphthoic acid). Table 3 also shows that complexes C_{10}COOBA-C_nOP have the most obvious monotropic mesophase behaviour in these systems. Additionally, by increasing the flexible length of the pyridine C_nOP (from $n = 8$ to $n = 16$) in complexes C_{10}COOBA-C_nOP and complexes C_{10}ONA-C_nOP, the mesomorphism shifts from the monotropic SmA phase or the enantiotropic nematic phase to the monotropic or enantiotropic SmC phase. These results indicate that simple H-bonded liquid crystals also follow the common rule that the SmC phase is more favoured in molecules with longer flexible lengths. In order to understand the fused-ring effects of the proton donors on the mesogenic properties of simple H-bonded complexes, complexes C_{10}OBA-C_nOP containing a single-ring (benzene) donor (C_{10}OBA) and complexes C_{10}ONA-C_nOP containing a fused-ring (naphthalene) donor (C_{10}ONA) in table 3 are compared. Significantly, the nematic phase is more favoured and higher clearing temperatures are expected in complexes C_{10}ONA-C_nOP due to the longer rigid core of the fused-ring (naphthalene) donor.

Table 2.   Phase transition temperatures (°C)[a] and corresponding enthalpies (J g^{-1}), in parentheses, of hydrogen-bonded complexes C_8OBA-C_8P, C_8OBA-C_8OP and C_8COOBA-C_8OP.

C_8OBA-C_8P[b]	Cr $\xrightarrow{45}$	N $\xrightarrow{49}$	I
C_8OBA-C_8OP	Cr $\underset{65.3\ (69.9)}{\overset{77.2\ (79.7)}{\rightleftarrows}}$	N $\underset{69.3\ (6.4)}{\overset{}{\rightleftarrows}}$	I
C_8COOBA-C_8OP	Cr $\underset{46.3\ (59.3)}{\overset{64.5\ (70.6)}{\rightleftarrows}}$	SmA $\underset{52.7\ (11.5)}{\overset{}{\rightleftarrows}}$	I

[a] Abbreviations: Cr = crystalline phase, SmA = smectic A phase, N = nematic phase, I = isotropic liquid.
[b] Data cited from reference [11].

Table 3. Phase transition temperatures (°C)[a] and corresponding enthalpies (J g^{-1}), in parentheses, of hydrogen-bonded complexes C$_{10}$OBA-C$_n$OP, C$_{10}$COOBA-C$_n$OP, C$_{10}$ONA-C$_n$OP and C$_{10}$COOTHA-C$_n$OP (where n = 8, 12 and 16).

Complex	Phase sequence (heating above / cooling below)
C$_{10}$OBA-C$_8$OP	Cr →66.6 (69.8) / ←57.0 (65.0) SmC →75.6 (7.5) / ←73.7 (7.0) I
C$_{10}$OBA-C$_{12}$OP	Cr →62.9 (33.6) / ←35.5 (22.0) SmX →65.1 (28.6) / ←53.0 (52.1) SmC →81.5 (25.0) / ←79.4 (30.4) I
C$_{10}$OBA-C$_{16}$OP	Cr →64.6 (50.6) / ←34.7 (12.8) Cr′ →39.6 (9.9) SmX →69.1 (13.5) / ←65.5 (13.0) SmC →83.3 (34.1) / ←82.4 (30.2) I
C$_{10}$COOBA-C$_8$OP	Cr →60.2 (65.3) / ←39.4 (63.9) SmA ←51.9 (3.2) I
C$_{10}$COOBA-C$_{12}$OP	Cr →74.1 (77.4) / ←60.7 (48.2) SmC ←61.3 (28.3) I
C$_{10}$COOBA-C$_{16}$OP	Cr →79.2 (90.9) / ←64.3 (59.6) SmC ←65.2 (31.0) I
C$_{10}$ONA-C$_8$OP	Cr →59.2 (58.0) / ←36.2 (45.5) N →96.8 (27.9) / ←94.9 (5.3) I
C$_{10}$ONA-C$_{12}$OP	Cr →48.0 (32.7) Cr′ →53.9 (14.7) Cr″ →60.9 (28.7) / ←35.4 (49.8) SmC →85.1 (5.8) / ←81.4 (2.1) N →93.6 (8.5) / ←92.7 (13.9) I
C$_{10}$ONA-C$_{16}$OP	Cr →67.7 (45.1) / ←34.2 (35.6) SmC →96.2 (17.1) / ←96.2 (15.7) I
C$_{10}$COOTHA-C$_8$OP	Cr →68.6 (55.8) / ←49.7 (25.5) Cr″ →52.9 (9.7) Cr′ →77.2 (56.6) / ←65.3 (66.6) I
C$_{10}$COOTHA-C$_{12}$OP	Cr →85.1 (99.8) / ←74.3 (101.4) I
C$_{10}$COOTHA-C$_{16}$OP	Cr →85.8 (111.1) / ←74.2 (112.1) I

[a] Abbreviations: Cr, Cr′, and Cr″ = crystalline phases, SmA = smectic A phase, SmC = smectic C phase, N = nematic phase, I = isotropic liquid.

The H-bonded dimer complexes bearing a fused-ring (IS) acceptor, i.e. C$_{10}$OBA-IS, C$_{10}$COOBA-IS, C$_{10}$ONA-IS and C$_{10}$COOTHA-IS (1:1 molar ratio) are shown in figure 3. Their thermal and mesogenic properties are given in table 4. The complex C$_{10}$COOTHA-IS, containing a thiophene proton donor, displays no

Table 4. Phase transition temperatures (°C)[a] and corresponding enthalpies (J g^{-1}), in parentheses, of hydrogen-bonded complexes C$_{10}$OBA-IS, C$_{10}$COOBA-IS, C$_{10}$ONA-IS and C$_{10}$COOTHA-IS from the 1:1 molar ratio of 6-dodecyloxyisoquinoline (IS) complexed with 4-decyloxybenzoic acid (C$_{10}$OBA), 4-decyloxycarbonylbenzoic acid (C$_{10}$COOBA), 6-decyloxy-2-naphthoic acid (C$_{10}$ONA) and 5-decyloxycarbonylthiophene-2-carboxylic acid (C$_{10}$COOTHA).

Complex	Phase sequence (heating above / cooling below)
C$_{10}$OBA-IS	Cr →83.8 (102.6) / ←62.1 (94.5) SmA →89.8 (15.9) / ←87.3 (13.6) I
C$_{10}$COOBA-IS	Cr →75.8 (93.8) / ←46.4 (78.5) SmA →78.8 (7.8) / ←73.5 (13.9) I
C$_{10}$ONA-IS	Cr →91.4 (66.9) / ←54.3 (60.5) SmA →102.5 (4.3) / ←100.5 (5.5) N →106.2 (3.8) / ←104.6 (4.1) I
C$_{10}$COOTHA-IS	Cr →83.2 (98.8) / ←67.7 (97.6) I

[a] Abbreviations: Cr = crystalline phases, SmA = smectic A phase, N = nematic phase, I = isotropic liquid.

liquid crystalline phase, which is also due to the short H-bonded angular structure. Except for C_{10}COOTHA-IS, all the other complexes in table 4, i.e. C_{10}OBA-IS, C_{10}COOBA-IS and C_{10}ONA-IS, possess the SmA phase, which might be due to the longer rigid core of the fused-ring proton acceptor (IS) in the complexes. Similarly to the comparison of complexes C_{10}OBA-C_nOP and C_{10}COOBA-C_nOP in table 3, complex C_{10}OBA-IS, containing the ether linkage in the proton donor, also has a higher clearing temperature and better mesomorphism than C_{10}COOBA-IS, containing the ester linkage in the proton donor. Since the flexible length of the fused-ring proton acceptor IS ($n = 12$) is equal to that of the single-ring proton acceptor C_{12}OP ($n = 12$), complexes C_{10}OBA-IS, C_{10}COOBA-IS and C_{10}ONA-IS in table 4 are analogous to C_{10}OBA-C_{12}OP, C_{10}COOBA-C_{12}OP and C_{10}ONA-C_{12}OP in table 3. In contrast to the latter systems containing the single-ring proton acceptor C_{12}OP as shown in table 3, the introduction of the fused-ring proton acceptor (isoquinoline) in C_{10}OBA-IS, C_{10}COOBA-IS and C_{10}ONA-IS, in general, has induced higher clearing temperatures due to the longer rigid core of the fused-ring (isoquinoline) acceptor structure. However, the ranges of the mesophases in these simple complexes are not improved by the fused-ring replacement in the proton acceptor. Although the nematic phase is observed in both C_{10}ONA-C_{12}OP and C_{10}ONA-IS, their mesomorphism has shifted from the enantiotropic or monotropic SmC phase in C_{10}OBA-C_{12}OP, C_{10}COOBA-C_{12}OP and C_{10}ONA-C_{12}OP to the enantiotropic SmA phase in C_{10}OBA-IS, C_{10}COOBA-IS and C_{10}ONA-IS. For single fused-ring systems, this suggests that the nematic phase is more favoured in simple H-bonded liquid crystals containing the fused-ring donor (naphthalene unit) systems, i.e. complexes C_{10}ONA-C_nOP (for $n = 8$ possessing the nematic phase 59.2–96.8°C and $n = 12$ possessing the nematic phase 85.1–93.6°C), rather than the fused-ring acceptor (isoquinoline unit) systems, i.e. complexes C_{10}OBA-IS (no nematic phase) and C_{10}COOBA-IS (no nematic phase). Hence, the fused-ring effect of the proton acceptors on the mesogenic properties of the simple H-bonded complexes is that the SmA phase is more favoured than the SmC phase; however, the fused-ring effect of the proton donors is that the nematic and the SmC phases are more favoured than the SmA phase. Overall, higher clearing temperatures are expected in the fused-ring systems than in single-ring systems.

For fused-ring acceptor systems in table 4, complex C_{10}ONA-IS containing the fused-ring acid has the highest clearing temperature and the best mesomorphism, and is the only structure to show the nematic phase. Nevertheless, in contrast to the double fused-ring complex C_{10}ONA-IS (containing both fused-ring donor and acceptor, i.e. naphthalene donor and isoquinoline acceptor), a single fused-ring (naphthalene donor) complex C_{10}ONA-C_{12}OP possesses better mesomorphism, i.e. wider ranges and lower phase transition temperatures of mesophases. The fused-ring effects on the mesogenic properties can be conceived by comparing analogous complexes containing double ether linkages, i.e. C_{10}OBA-C_{12}OP (no fused-ring system, possessing the SmC phase 65.1–81.5°C), C_{10}ONA-C_{12}OP (single fused-ring donor system possessing the SmC phase 60.9–85.1°C and the nematic phase 85.1–93.6°C), C_{10}OBA-IS (single fused-ring acceptor system possessing the SmA phase 83.8–89.8°C) and C_{10}ONA-IS (double fused-ring system possessing the SmA phase 91.4–102.5°C and the nematic phase 102.5–106.2°C). The results of this comparison are summarized as follows: Firstly, the greater the number of fused-ring structures in the H-bonded complexes, the higher the clearing temperature that will be obtained. Secondly, the ranges of the useful mesogenic phases, including nematic, SmA and SmC, are in the following order: C_{10}ONA-C_{12}OP (single fused-ring donor system) > C_{10}OBA-C_{12}OP (no fused-ring system) > C_{10}ONA-IS (double fused-ring system) > C_{10}OBA-IS (single fused-ring acceptor system). Finally, the SmC phase is favoured in the single-ring acceptor systems (C_{10}OBA-C_{12}OP and C_{10}ONA-C_{12}OP); the nematic phase is favoured in the fused-ring donor systems (C_{10}ONA-C_{12}OP and C_{10}ONA-IS); the SmA phase is favoured in the fused-ring acceptor systems (C_{10}OBA-IS and C_{10}ONA-IS).

To prove the formation of H-bonded architecture, XRD patterns were measured to confirm our speculation. Since the molecules are orthogonal to the layer in the SmA phase, the largest *d*-spacing values of the SmA phase are correlated to the length of the supramolecules. Table 5 shows the *d*-spacing values in the SmA phase of complexes C_{10}OBA-IS, C_{10}COOBA-IS and C_{10}ONA-IS. The lengths of each component calculated by molecular modelling are listed as follows: C_{10}OBA = 19.1 ∼ 20.6 Å, C_{10}COOBA = 20.2 ∼ 21.8 Å, C_{10}ONA = 21.3 ∼ 22.8 Å and IS = 20.0 ∼ 23.2 Å; the former value is the molecular projection length along the rigid core and the latter value is the fully extended molecular length. According to the XRD patterns, complexes C_{10}OBA-IS, C_{10}COOBA-IS and C_{10}ONA-IS have the largest *d*-spacing values 40.19 Å at 70°C (cooling), 40.45 Å at 68°C (cooling) and 42.84 Å at 96°C (heating), respectively. Both C_{10}OBA-IS and C_{10}COOBA-IS have similar largest *d*-spacing values, which are close to the sum (∼ 40 Å) of each component. Hence, they are approximately the same length in their supramolecular configurations. C_{10}COOBA-IS is a little larger than C_{10}OBA-IS, owing to the longer ester linking group in C_{10}COOBA-IS compared with the shorter ether linking group in C_{10}OBA-IS.

Table 5. The *d*-spacing values of H-bonded complexes $C_{10}OBA$-IS, $C_{10}COOBA$-IS and $C_{10}ONA$-IS in the SmA phase obtained from XRD measurements at different temperatures.

Complex		Temperature/°C[a]	*d*-spacing/Å
$C_{10}OBA$-IS	(Heating)	82	39.62
		84	39.42
		86	39.33
		88	39.22
	(Cooling)	85	39.46
		80	39.68
		75	39.81
		70	40.19
$C_{10}COOBA$-IS	(Heating)	76	39.77
		78	39.43
	(Cooling)	73	40.11
		70	40.15
		68	40.45
$C_{10}ONA$-IS	(Heating)	94	42.43
		96	42.84
		98	42.71
		100	42.60
	(Cooling)	100	41.06
		90	40.77
		80	41.18
		70	41.31

[a] All temperatures reported were first measured at a heating scan to the clearing temperature and then followed a cooling scan to room temperature. Small temperature deviations from DSC data may occur due to the annealing effect in XRD measurements.

Significantly, $C_{10}ONA$-IS has the largest *d*-spacing value due to its longest double fused-ring core containing both H-bonded naphthalene and isoquinoline units. As with normal mesogenic materials, most *d*-spacing values of the SmA phase decrease as the temperature increases. Generally, the *d*-spacing data match the calculated molecular lengths from molecular modelling, and the XRD results confirm their supramolecular structures.

4. Conclusions

In conclusion, the distinct liquid crystalline properties of new simple supramolecular structures are evident and introduced by the H-bonded single-ring or fused-ring donors and acceptors. XRD measurements have confirmed their novel molecular architectures. None of the complexes containing thiophene, i.e. $C_{10}COOTHA$-C_nOP and $C_{10}COOTHA$-IS, exhibit any liquid crystalline phase, which is due to the short H-bonded angular structure. From this study, we can verify that the linking group has not only influenced the formation of the H-bonded liquid crystals (unless there is phase separation) but has also affected the type of the mesophase. In general, the clearing temperatures of analogous complexes containing different linking groups are in the following order: alkoxyl chains > alkyl ester chains > alkyl chains. The result of this investigation also implies that the fused-ring structures in H-bonded complexes can have a variable influence on the mesomorphism, depending on the fused-ring structures being on the proton side or on the acceptor side (or on both sides) of the complex. Consequentially, the naphthalene- and isoquinoline-based structures supply fused-rings as the proton donor and acceptor to form unique supramolecules. Overall, this study has illustrated a simple H-bonded molecular architecture in the design of supramolecular liquid crystals. Through this research, the fused-ring and linking group effects on simple supramolecular liquid crystals can be visualized, and similar effects might be expected in general H-bonded liquid crystals. By the adjustment of fused-ring structures and linking groups in H-bonded moieties, it is possible to create interesting mesomorphism in novel supramolecular liquid crystals.

References

[1] LEHN, J. M., 1988, *Angew. Chem. int. Ed. Engl.*, **27,** 89.
[2] DESIRAJU, G. R., 1995, *Angew. Chem. int. Ed. Engl.*, **34,** 2311.
[3] KATO, T., and FRÈCHET, J. M. J., 1989, *J. Am. chem. Soc.*, **111,** 8533.
[4] KATO, T., FUJISHIMA, A., and FRÈCHET, J. M. J., 1990, *Chem. Lett.*, 919.
[5] KATO, T., FRÈCHET, J. M. J., WILSON, P. G., SAITO, T., URYU, T., JIN, C., and KANEUCHI, F. M. J., 1993, *Chem. Mater.*, **5,** 1094.
[6] PALEOS, C. M., and TSIOURVAS, D., 1995, *Angew. Chem. int. Ed. Engl.*, **34,** 1696.
[7] WALLAGE, M. J., and IMRIE, C. T., 1997, *J. mater. Chem.*, **7,** 1163.
[8] KAWAKAMI, T., and KATO, T., 1998, *Macromolecules*, **31,** 4475.
[9] KATO, T., IHATA, O., UJIIE, S., TOKITA, M., and WATANABE, J., 1998, *Macromolecules*, **31,** 3551.
[10] LIN, H. C., LAI, L. L., LIN, Y. S., TSAI, C., and CHEN, R. C., *Mol. Cryst. liq. Cryst.* (in the press).
[11] FUKUMASA, M., KATO, T., URYU, T., and FRÈCHET, J. M. J., 1993, *Chem. Lett.*, 65.
[12] LAI, L. L., WANG, C. H., HSIEH, W. P., and LIN, H. C., 1996, *Mol. Cryst. liq. Cryst.*, **287,** 177.
[13] LIN, H. C., LAI, L. L., HSIEH, W. P., and HUANG, W. Y., 1997, *Liq. Cryst.*, **22,** 661.
[14] TSO, H. H., WANG, J. S., WU, C. Y., and LIN, H. C., 1998, *New J. Chem.*, 771.

[15] LIN, H. C., KO, C. W., GUO, K., and CHENG, T. W., 1999, *Liq. Cryst.*, **26,** 613.
[16] LIN, H. C., and LIN, Y. S., 1998, *Liq. Cryst.*, **24,** 315.
[17] LIN, H. C., LIN, Y. S., LIN, Y. S., CHEN, Y. T., CHAO, I., and LI, T. W., 1998, *Macromolecules*, **31,** 7298.
[18] LIN, H. C., SHIAW, J. M., LIU, R. C., TSAI, C., and TSO, H. H., 1998, *Liq. Cryst.*, **25,** 277.

[19] COHEN, J. B., and DE PENNINGTON, H. S., 1918, *J. chem. Soc.*, **113,** 63.
[20] STEPANOV, F. N., and VERETENOVA, T. N., 1965, *J. org. Chem. USSR (Engl. Transl.)*, **1,** 1414.
[21] GRAY, G. W., and JONES, B., 1954, *J. chem. Soc.*, 678.
[22] HENDRICKSON, J. B., and RODRÌGUEZ, C., 1983, *J. org. Chem.*, **48,** 3344.